J. Astron. Space Sci. 12(2), 168–178 (1995)

MODEL DUST ENVELOPES FOR ASYMPTOTIC GIANT BRANCH STARS. II. CARBON STARS

Kyung-Won Suh and Hee-Joung Kwoun
Department of Astronomy and Space Science, Chungbuk National University
e-mail: kwsuh@astro.chungbuk.ac.kr

(Received September 28, 1995; Accepted October 20, 1995)

ABSTRACT

We have modeled the dust envelopes around carbon stars with close attention to the evolution of the structure of the dust shells. We use various dust density distributions to take account the effect of the superwind due to the helium shell flash by adding a density increased region. Depending on the position and quality of the density increased region, the model results are different from the results with conventional density distribution. The new results fit the observations of some carbon stars better. The IR two-color diagrams comparing the results of the super wind models and IRAS observation of 252 carbon stars have been made. The new results can explain much wider regions on the IR two-color diagrams.

1. INTRODUCTION

Carbon stars are believed to be the evolutionary successors of M-type Mira variables that have thin oxygen-rich dust envelopes. When the intermediate mass range asymptotic giant branch stars go through the carbon dredge-up, oxygen-rich grains cease from forming and the mass loss stops temporarily and becomes visual carbon stars. After that phase, carbon grains start forming and they become infrared carbon stars with thick carbon dust envelopes and very high mass loss rates (*e.g.*, Iben 1981, Kwok *et al.* 1989). As asymptotic giant branch (AGB) stars evolve to planetary nebulae, thermal pulses due to sporadic helium shell flashes have been considered to be one of the major cause of increasing mass loss. In this paper, we investigate the influence of the superwind on the spectral energy distribution of carbon stars. We modify the dust density distribution by adding a density increased region. We try to simulate the influence of the superwind using above method and to compare in detail the new results with previous model results and the observed spectral energy distribution (SED) of the carbon stars.

2. PROCEDURES OF RADIATIVE TRANSFER MODEL CALCULATIONS

We have used Leung's radiative transfer code (Egan *et al.* 1988) for spherical symmetric dust shells. In the present calculations, a radial grid of 125 points and a wavelength grid of 90 points were used. The scattering is accurately considered. The radiation from a central hot source hits the inner part of the dust shells around it and the dust grains redistribute the energy spectra continuously toward longer wavelength bands.

For the dust envelope, we have adopted the absorption and scattering efficiency factors as described in the last section. The radii of spherical dust grains have been assumed to be 0.1 μm uniformly. The dust condensation temperature (T_c) is assumed to be 1000 K and the dust condensation radius (R_c) is obtained after a few trials. The outer radius of the dust shell is always taken to be 1000 R_c. Finally, the dust optical depth at 10 μm ($\tau_{\lambda=10\mu m}$) is taken to fit the observations of each object. Their typical values are in the range of 0.05 - 1.0.

For the central hot source, the luminosity is taken to be $5.8 \times 10^4 L_\odot$ and the black body temperature of 2000 K is assumed. The change of the luminosity does not affect the shape of the output spectra very much, it only affects the overall energy output throughout wide wavelength ranges. The change of the central blackbody temperature does affect the output spectra. But the minor temperature changes between 2000 K and 3000 K do not make much difference.

2.1 Dust Opacity

The chemical composition of dust grains in the envelopes of carbon stars is not very well known. The graphite particles that are believed to comprise of most carbon rich interstellar dust do not fit carbon stars any way. Instead, amorphous carbon grains (probably with a minor mixture of SiC and other materials) appear to be the best candidate. Draine & Lee (1984) suggested graphite, Rowan-Robinson & Harris (1983) suggested amorphous carbon, and Gehrz (1989) suggested SiC. Some authors suggested a mixture of multiple grain materials. After testing various grain materials by the radiative transfer model calculations and the close comparison with observations that we will discuss in the next section, we have found that the amorphous carbon (AMC) with slight modification in the far-infrared band is the best choice.

We have used the optical constants for amorphous carbon measured by Duley (1984) in visible band (λ = 0.2 - 0.7 μm). Koike *et al.* (1980) found a Rayleigh scattering pattern in near-infrared band (λ = 0.7 - 7 μm). And in the far-infrared band (λ = 7 - 100 μm), we have tested a simple extension of Rayleigh scattering and a slight modification. As we will discuss in the next section, we find that the slight modification improves the fitting with observations. Figure 1 shows the opacity pattern of the modified amorphous carbon that

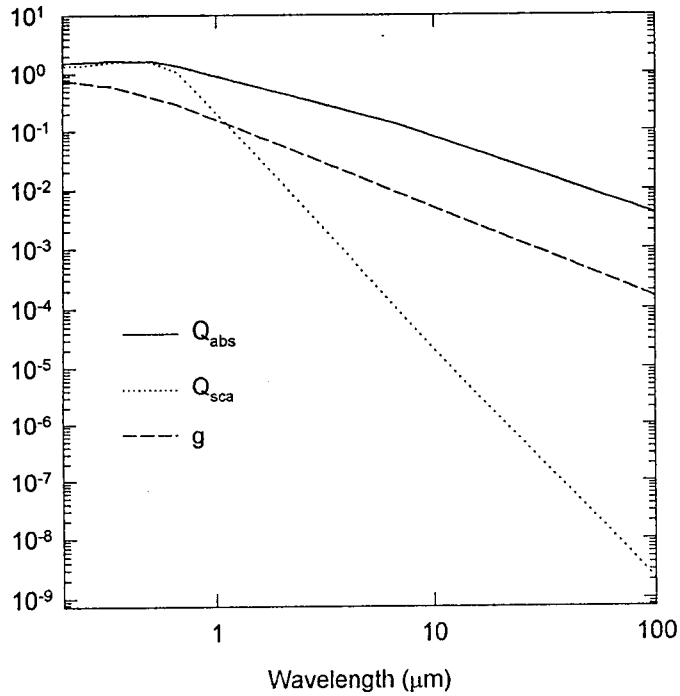

Figure 1. Absorption and Scattering efficiency factors.

we have used for modeling infrared carbon stars. The absorption and scattering efficiency factors (Q_{abs}, Q_{sca}) and the anisotropy factors (g = $< \cos\theta >$; where θ is the angle between the incident wave and the scattered wave) are very different.

2.2 Dust Density Distribution

According to the classical nucleation theory, the final grain size is calculated to be about 0.1 μm and dust formation and growth time-scales are much shorter than those for OH/IR stars (*e.g.*, Suh 1990) which is very short compared with other time scales for typical carbon stars' environments. This burst-like grain formation suggests overall constant outflow (*i.e.*, the density distribution is $\rho(r) \propto r^{-2}$). The dust density distributions are usually assumed to be inversely proportional to the square of the distance.

But if we take the effects of the superwinds into account, the dust density distribution should be different from the smooth distribution. We expect one thermal pulse per each $10^4 - 10^5$ years which endure for about 100-1000 years. The dust condensation radius from the center of the central star (R_c) is about 0.1×10^{-3} pc for typical carbon stars. The

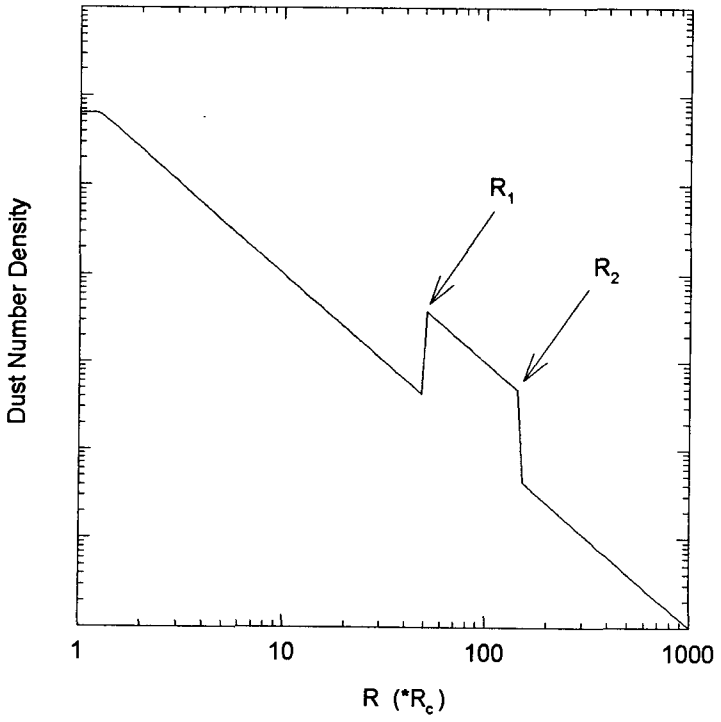

Figure 2. Dust Density Distribution.

expansion velocity is about 10 - 20 km/sec. A change in the dust density distribution will affect the outgoing spectra. The effect will be different depending on the location of the change, and the change up to 1000 R_c will do affect the outgoing energy spectra. The travel time for 1000 R_c is about 6000 years which is smaller than thermal pulse period. So there should be only one discontinuity. We may expect that a significant portion of AGB stars have that discontinuity in their dust shells. And we may expect that about a half of the AGB stars have the discontinuity in their dust shells at various radii. The shape of discontinuity in the dust density distribution would be like figure 2. The density suddenly increases at R_2 then goes back to initial state at R_1.

3. SPECTRAL ENERGY DISTRIBUTION COMPARISON

The SEDs of many carbon stars are collected from various sources. Especially the third catalog of infrared observations (Gezari *et al.* 1993) has been very useful. The observational data are from many references for last 20 years of infrared observations of

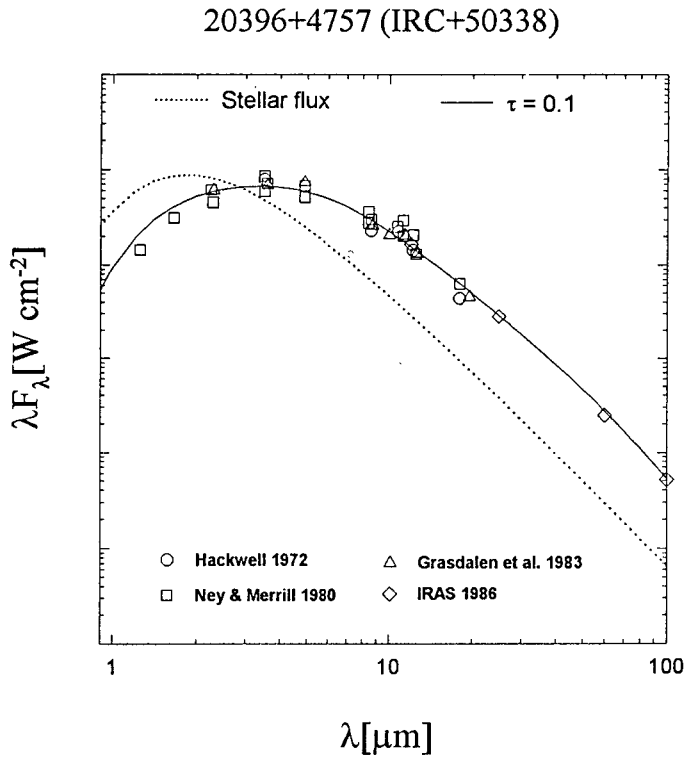

Figure 3. Model Results compared with Observations for IRC+50338.

Carbon stars. We have obtained the results of model calculations with various possible stellar and dust envelope parameters. The results are compared with observations and more reliable input parameters are obtained. The data are mostly in infrared magnitudes or Jansky unit. They are converted to an absolute flux unit (λF_λ; Watts/cm^2) by zero magnitude calibration processes using the instrument's characters mentioned in each paper (see e.g., Gehrz *et al.* 1987).

We have compared the results with the observed SEDs of the following carbon stars in detail; IRC+50338, IRC+50096, IRC+30374, AFGL 2686, IRC+40540, IRC+10216. For SED comparison, the theoretical model calculations use the continuous dust density distribution ($\rho(r) \propto r^{-2}$).

Figure 3 shows the results of the model calculations (lines) superimposed on observational data (symbols) for IRC+50338. The observational data from Hackwell (1972) are shown as circles, Grasdalen *et al.* (1983) as triangles, Ney and Merrill (1980) as squares, and IRAS (1986) as diamonds, respectively. Figure 4 shows the results of the model

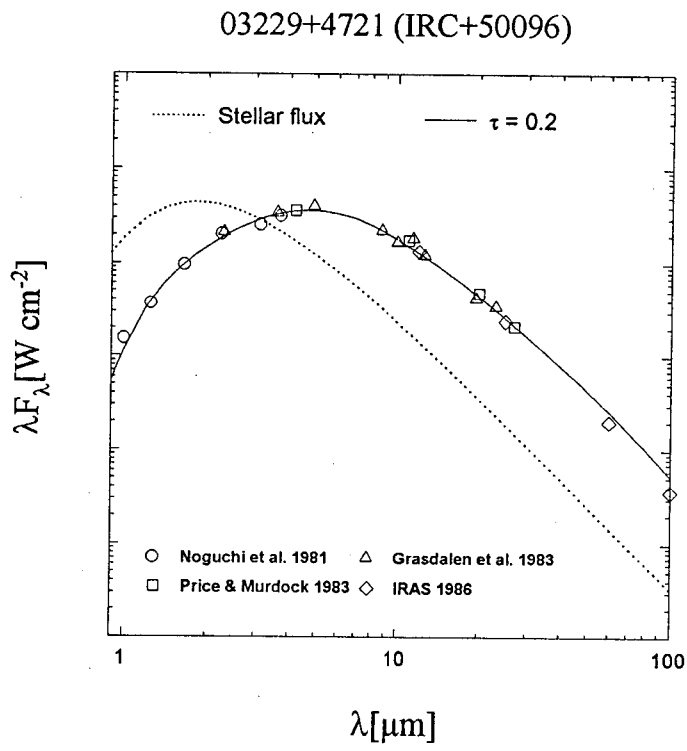

Figure 4. Model Results compared with Observations for IRC+50096.

calculations (lines) superimposed on observational data (symbols) for IRC+50096. The observational data from Noguchi *et al.* (1981) are shown as circles, Grasdalen *et al.* (1983) as triangles, Price & Murdock (1983) as squares, and IRAS(1986) as diamonds, respectively. Figure 5 shows the results of the model calculations (lines) superimposed on observational data (symbols) for IRC+30374. The observational data from Merrill and Stein (1976) are shown as circles, Grasdalen *et al.* (1983) as triangles, Noguchi *et al.* (1981) as squares, and IRAS(1986) as diamonds, respectively. Figure 6 shows the results of the model calculations (lines) superimposed on observational data (symbols) for AFGL 2686. The observational data from Gosnell *et al.* (1979) are shown as circles, and IRAS(1986) as diamonds, respectively. Figure 7 shows the results of the model calculations (lines) superimposed on observational data (symbols) for AFGL IRC+40540. The observational data from Strecker & Ney (1981) are shown as circles, Grasdalen *et al.* (1983) as trianglesas, Merrill and Stein (1976) as squares, and IRAS (1986) as diamonds, respectively. Figure 8 shows the results of the model calculations (lines) superimposed on observational data (symbols) for IRC+10216. The observational data from Strecker & Ney (1974) are shown as circles,

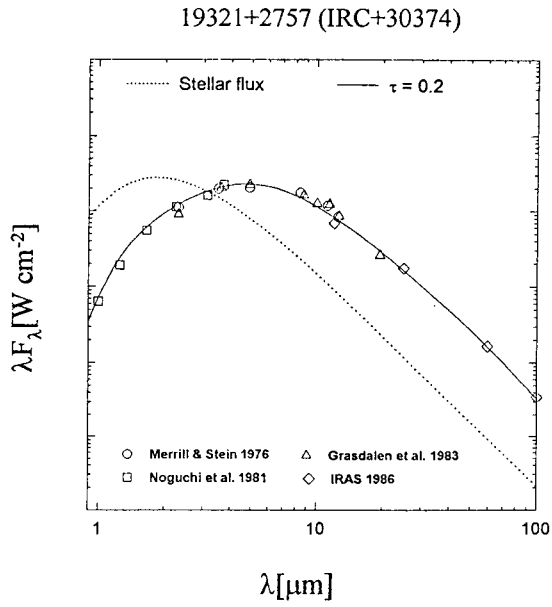

Figure 5. Model Results compared with Observations for IRC+30374.

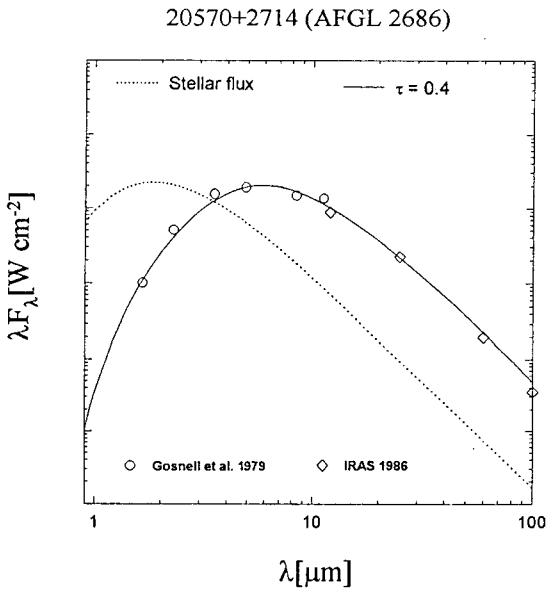

Figure 6. Model Results compared with Observations for AFGL 2686.

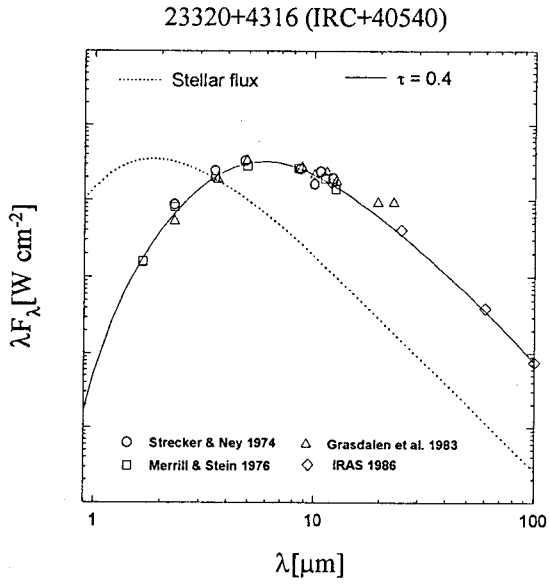

Figure 7. Model Results compared with Observations for IRC+40540.

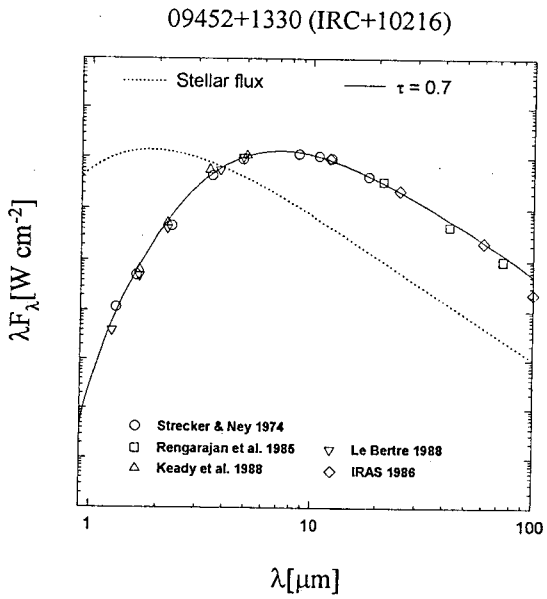

Figure 8. Model Results compared with Observations for IRC+10216.

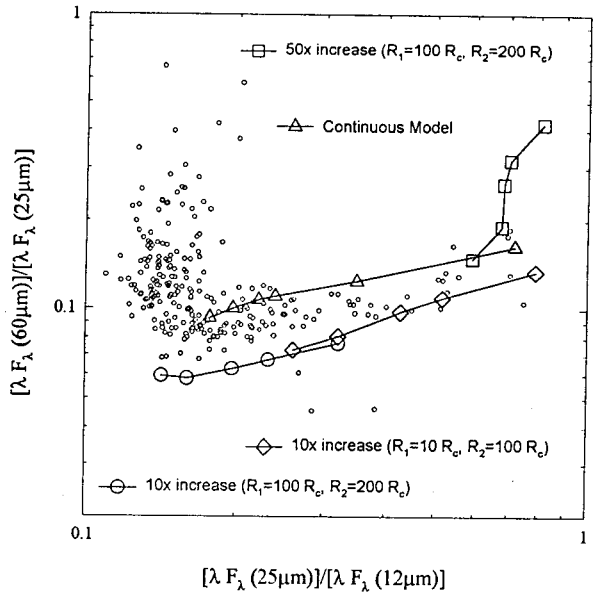

Figure 9. Model Results compared with IRAS Observations on IR 2-color Diagram.

Rengarajan *et al.* (1985) as squares, Le Bertre (1988) as down triangles, Keady *et al.* (1988) as up triangles, and IRAS (1986) as diamonds, respectively.

We find that the models with the modified amorphous carbon make good overall fittings. The modified amorphous carbon grains fit all model stars with almost the same accuracy regardless their total optical depth. We do not find any systematic deviations depending on the total optical depth.

4. COMPARISON ON IRAS 2-COLOR DIAGRAMS

IRAS 4-color photometric data are available for 252 carbon stars. (Egan & Leung 1991, Chan 1993, Volk *et al.* 1992, Volk *et al.* 1993, Groenewegen 1995, Groenewegen *et al.* 1995). In figure 9, small circles represent observational data. The points in the far left-hand corner shows the positions of optical carbon stars which are out of scope of this work, while the other points shows the positions of infrared carbon stars. The lines and big symbols in figure 9 represent the model calculation results with various optical depths including the superwind models.

As optical depth increases the model result positions on the 2-color diagram move toward upper-right corner. Continuous (conventional) models do not cover wide regions of

observational data while the superwind models do. Depending on the location and quality of the discontinuity the positions on the 2-color diagram change. The superwind model results can explain the various positions on the IR 2-color diagram of carbon stars.

5. DISCUSSION

The effect of temperature on the optical properties of dust has been noted by a number of authors (*e.g.*, Volk & Kwok 1988, Suh 1991) for circumstellar silicate grains. They find that the deduced opacities at longer wavelengths ($\lambda > 12\mu$m) for OH/IR stars are higher than the one for M-type Miras possibly because of the change of optical constants depending on the temperature of dust grains. And Colangeli *et al.* (1992) have found the similar temperature effect of opacity for hydrogenated amorphous carbon and polycyclic aromatic hydrocarbon molecules in their laboratory experiments. But contrary to our expectation, we do not find such variations for amorphous carbon showing uniform fitting for various dust optical depths with only one dust opacity pattern.

The superwind model results fit the IRAS observations of some carbon stars better. So we may conclude that the superwind models should be incorporated for considerable portion of carbon stars. The more detailed model comparison would reveal further effects of superwinds on the SEDs of infrared carbon stars.

ACKNOWLEDGMENTS: This paper was supported by the Basic Science Institute Program, Ministry of Education, 1995, Project No. BSRI-95-5413.

REFERENCES

Chan, S. J. 1993, PASP, 105, 1107
Colangeli, L., Mannela, V. & Bussoletti, E. 1992, ApJ, 385, 577
Draine, B. T. & Lee, H. M. 1984, ApJ, 285, 89.
Duley, W. W. 1984, ApJ, 287, 694
Egan, M. P., Leung, C. M. & Spagna, G. F., Jr. 1988, Computer Phy. Comm., 48, 271
Egan, M. P. & Leung, C. M. 1991, ApJ, 383, 314
Gehrz, R. D. 1989, in IAU Symp. 135, Interstellar Dust, L. J. Allamandola & A. G. G. M. Tielens, Dordrecht: Kluwer, 445
Gehrz, R. D., Grasdalen, G. L. & Hackwell, J. A. 1987, in The Encyclopedia of Physical Science and Technology, 2, 53
Gezari, D. Y., Schmitz, M., Pitts, P. S. & Mead, J. M. 1993, Catalog of Infrared Observations, Third Edition, NASA Reference Publication 1294

Gosnell, T. R., Hudson, H. S. & Puetter, R. C. 1979, AJ, 84, 538
Grasdalen, G. L., Gehrz, R. D., Hackwell, J. A., Castelaz, M. & Gullixson, C. 1983, ApJS, 53, 413
Groenewegen, M. A. T. 1995, A&A, 293, 463
Groenewegen, M. A. T., van den Hoek, L. B. & de Jong, T. 1995, A&A, 293, 381
Hackwell, J. A. 1972, A&A, 21, 239
Iben, I. 1981, ApJ, 246, 278
IRAS catalogues and atlases 1986, Point Source Catalogue, US Government Publication Office
Keady, J. J., Hall, D. N. B. & Ridgway, S. T. 1988, ApJ, 326, 832
Koike, C., Hasegawa, H. & Manabe, A. 1980, Ap&SS, 67, 495
Kwok, S., Volk, K. M. & Chan, S. J., 1989, *in Evolution of Peculiar Red Giant Stars,* ed. H. R. Johnson & B. Zuckerman (Cambridge: Cambridge University Press), p.284
Le Bertre, T. 1988, A&A, 203, 85
Merrill, K. M. & Stein, W. A. 1976, PASP, 88, 294
Ney, E. P. & Merrill, K. M. 1980, AFGL-TR-80-0050, US Government Publication Office
Noguchi, K., Kawara, K., Kobayashi, Y., Okuda, H., Sato, S. & Oishi, M. 1981, PASJ, 33, 373
Price, S. D. & Murdock, T. L. 1983, AFGL-TR-83-0161, US Government Publication Office
Rengarajan, T. N., Fazio, G. G., Maxson, C. W., McBreen, B., Serio, S. & Sciortino, S. 1985, ApJ, 289, 630
Rowan-Robinson, M. & Harris, S. 1983, MNRAS, 202, 797
Strecker, D. W. & Ney, E. P. 1974, AJ, 79, 1410
Suh, K. W., Jones, T. J. & Bowen, G. H. 1990, ApJ, 358, 588
Volk, K., Kwok, S. & Langill, P. P. 1992, ApJ, 391, 285
Volk, K., Kwok, S. & Woodsworth, A. W. 1993, ApJ, 402, 292